Genotoxic stress abrogates renewal of melanocyte stem cells by triggering their differentiation.

doi: 10.1016/j.cell.2009.03.037

Cell, Volume *137*

Supplemental Data

Genotoxic Stress Abrogates Renewal of Melanocyte Stem Cells by Triggering Their Differentiation

Ken Inomata, Takahiro Aoto, Nguyen Thanh Binh, Natsuko Okamoto, Shintaro Tanimura, Tomohiko Wakayama, Shoichi Iseki, Eiji Hara, Takuji Masunaga, Hiroshi Shimizu, and Emi K. Nishimura

Supplemental Experimental Procedures

Animals

C57BL/6J mice were purchased from Sankyo Lab Service. Animal care was in accordance with the guidance of Kanazawa University for animal and recombinant DNA experiments. All animal experiments were performed following the Guidelines for the Care and Use of Laboratory Animals, and were approved by the Committee of Laboratory Animal Experimentation in Kanazawa University. Offspring were genotyped by PCR-based assays of mouse tail DNA and wild-type littermates were used as controls in all experiments.

Histology and Immunohistochemistry

For paraffin sections, mouse skins were fixed in 10% formalin solution at 4 °C overnight.

For whole mount β-galactosidase staining, the fixed samples were stained in 5-bromo-4-chloro-3-indolyl-β-D-galactoside solution (X-gal) (Invitrogen), post-fixed in 10% formalin solution, and embedded in paraffin. Paraffin-embedded skin specimens were cut in 5

μm-thick sections (Rotary Microtome HM325, MICROM International GmbH.). Sections were deparaffinized, rehydrated, and stained with hematoxylin-eosin (Sakura Finetechnical Co. Ltd.) or Fontana-Masson silver stain (Diagnostic BioSystems) for analysis of tissue histology using a microscope. For antigen retrieval, sections were microwave heated at 90°C in Target retrieval solution (DAKO) for 20 min prior to immunostaining. Nonspecific staining was blocked by pre-incubation with phosphate-buffered saline (PBS) containing 3% skim milk (Difco) for 30 min. Tissue sections were incubated with the primary antibody at 4°C overnight, and were subsequently incubated with biotinylated goat anti-mouse or anti-rabbit immunoglobulin G antibody (Vector Laboratories) at room temperature for 30 min. After washing, the sections were incubated with avidin-biotin peroxidase complex using the Vectastain Elite ABC kit (Vector Laboratories) at room temperature for 30 min. After color development with 3,3-diaminobenzidine as the substrate, sections were counterstained with hematoxylin. Coverslips were mounted onto glass slides with mounting media (Daidosangyo Co., Ltd.). Images were obtained with an upright microscope BX51 (Olympus).

Immunofluorescence

Pieces of fresh mouse dorsal skin were immersed in ice-cold 4% paraformaldehyde (PFA) in PBS (pH 7.4), and were irradiated in a 500W microwave oven for three 30-sec cycles with intervals. The fixed skin samples were embedded in OCT compound (Sakura Finetechnical Co. Ltd.), snap-frozen in liquid nitrogen, and stored at –80°C. Frozen samples were cut in 10 μm-thick sections (Cryomicrotome CM 1850, Leica Microsystems Nusslch GmbH.), and were used for immunofluorescence analysis. Nonspecific staining was blocked by incubation with PBS containing 3% skim milk (Difco) for 30 min. Tissue sections were incubated with the primary antibody at 4°C overnight, and were subsequently incubated with secondary antibodies

conjugated with Alexa Fluor 488, 568 or 594 (Invitrogen). After washing in PBS, 4',6-diamidine-2'-phenylindole dihydrochloride (DAPI, Invitrogen) was added for nuclear counterstaining. Coverslips were mounted onto glass slides with fluorescent mounting medium (Thermo Electron Corp.). All images were obtained using an upright microscope BX51 (Olympus), or on FV1000 confocal microscope system (Olympus).

Antibodies

For immunohistochemistry, the following antibodies were used: rabbit anti-β-galactosidase (1:300, Cappel), rabbit anti-phospho histone H2AX (1:100, Cell Signaling), rabbit anti-53BP1 (1:300, Lifespan BioSciences), rabbit anti-ATM (1:200, Rockland), rabbit anti-phospho-ATM (1:200, Rockland), rabbit anti-Ki67 (1:300, NovoCastra), chicken anti-keratin 15 (1:300, Covance), biotin anti-mouse CD11b (1:100, eBioscience), rabbit anti-cleaved caspase 3 (1:300, Cell Signaling), mouse anti-p16 (1:100, Santa Cruz Biotechnology, Inc.), rabbit anti-p53 (1:500, NovoCastra) and rat anti-mouse CD117 (1:200, BD Pharmingen). Mouse anti-MITF antibody (C5) was a kind gift from Dr. David Fisher, Dana Farber Cancer Center (Hemesath et al., 1998). Rabbit anti-Tyrp1 (PEP1) and rabbit anti-Tyrosinase (PEP7) were kind gifts from Dr. Vincent Hearing, National Cancer Institute (Jimenez et al., 1989; Tsukamoto et al., 1992).

Cell culture, X-ray irradiation, and image analysis

Normal human epidermal melanocytes (NHEM) were purchased from Kurabo, and were maintained in Medium 254 containing Human Melanocyte Growth Supplement (bovine pituitary extract, 0.2%; fetal bovine serum, 0.5%; bovine insulin, 5 μg/ml; bovine transferrin, 5 μg/ml; basic fibroblast growth factor, 3 ng/ml; hydrocortisone, $5x10^{-7}$ M; heparin, 3 μg/ml; phorbol 12-myristate 13-acetate, 10 ng/ml;), penicillin (100 U/ml), streptomycin (100 μg/ml), and

amphotericin (250 ng/ml), all from Kurabo) in a humidified atmosphere with 5% CO_2 at 37^{o}C. IR (3.0 Gy/min) was administered using a Faxitron RX-650 (130 kVp and 5 mA, Faxitron X-ray Corp.). Cells were exposed to different doses (5 and 10 Gy) of IR, and morphological changes were observed by light microscopy (IX71, Olympus). SA-β-Gal staining was performed using a commercial kit (Sigma-Aldrich), following the manufacturer's instructions. γH2AX foci were detected by immunostaining with anti-phospho histone H2AX antibody, and images were obtained using an upright microscope BX51 (Olympus).

Supplemental References

Hemesath, T.J., Price, E.R., Takemoto, C., Badalian, T., and Fisher, D.E. (1998). MAP kinase links the transcription factor Microphthalmia to c-Kit signalling in melanocytes. Nature *391*, 298-301.

Jimenez, M., Maloy, W.L., and Hearing, V.J. (1989). Specific identification of an authentic clone for mammalian tyrosinase. J. Biol. Chem. *264*, 3397-3403.

Tsukamoto, K., Jackson, I.J., Urabe, K., Montague, P.M., and Hearing, V.J. (1992). A second tyrosinase-related protein, TRP-2, is a melanogenic enzyme termed DOPAchrome tautomerase. Embo J. *11*, 519-526.

Figure Legends

Figure S1. Schematic figure of MSC behavior during the hair cycle.

MSCs (blue) are maintained in the lowest permanent portion (P) throughout the hair cycle. MSCs are activated to divide only at early anagen to supply transit amplifying progeny (TA: red) to the hair matrix, where they mature into differentiated melanocytes (MM: green). After stem cell division, stem cell progenies are retained in the bulge area and reenter the quiescent (non-cycling) state. Abbreviations: P, permanent portion; T, transient portion; MSC, melanocyte stem cell; TA, transit amplifying cell; MM, mature melanocyte.

Figure S2. MSCs remain quiescent for at least 24 hours after hair plucking.

Immunohistochemical analysis of Ki67 expression (brown) by Dct-lacZ$^+$ cells (blue) in the hair follicle bulge (a-c). Insets show magnified images of the Dct-lacZ$^+$ cells indicated by the arrowheads. The scale bar represents 25 μm in (c) and 10 μm in the inset of (c).

Figure S3. Telogen-to-anagen progression is required for EPM induction and hair graying.

a-f, Changes in coat colors of control (a-c) and irradiated mice (d-f) at 3, 7 and 16 weeks of age without hair plucking. Mice were irradiated at 3-weeks-old when the hair follicles on the dorsal skin are naturally synchronized at telogen. This reproducibly induced irreversible hair graying on the trunk even after hair molting (e, f).

g-j, EPMs appear in the niche only after hair follicles have entered anagen phase. LacZ stained sections of *Dct-lacZ* transgenic mice irradiated at 7 weeks after birth when their hair is naturally synchronized at telogen (this method is termed "telogen-IR") (g, i), after which anagen was induced by hair depilation at 1 week after telogen-IR (h, j). In this experiment, telogen-IR was performed without any prior hair plucking. **g, i,** Dct-lacZ$^+$ cells remain unpigmented and

quiescent in the bulge areas of telogen hair follicles even after 1 week after telogen-IR (i) and in the non-irradiated control (g). **h, j**,. Dct-lacZ^{+} cells in the hair follicle bulge areas of anagen IV. Dct-lacZ^{+} cells are dendritic and ectopically pigmented in irradiated follicle, but not in control (j, arrowhead). Scale bars represent 25 μm in (j) and 10 μm in the inset of (j).

Figure S4. EPMs eventually disappear from the niche at anagen VI.

Immunohistochemical staining of anagen hair follicles for K15 (keratin 15, a bulge keratinocyte marker) (green) and for KIT (red). The bulge areas of control follicles at anagen VI (a-c), and of irradiated hair follicles at anagen V (d-f) and anagen VI (g-i) are shown. Merged images of bright field views (c, f, and i) and immunostaining (b, e, h) are shown in (a), (d) and (g), respectively. Insets show magnified images of the KIT^{+} melanoblasts/melanocytes marked with arrowheads. **a-c**, KIT^{+} melanoblasts in the bulge areas of control anagen VI follicles (a, b, white arrowheads) did not contain any melanin pigment in the bright field view (c, arrowhead**). d-f,** KIT^{+} EPMs in the bulge areas of irradiated follicles at anagen V. EPMs are dendritic and contain abundant pigment in the cytoplasm (f, arrowhead). **g-i,** KIT^{+} EPMs were absent in the bulge areas and residual pigment (arrows) was found in the cytoplasm of K15^{+} keratinocytes in the bulge areas (hair follicle stem cells). The residual pigments and low levels of KIT signals were sometimes found in K15-expressing keratinocytes in the bulge areas prior to the complete disappearance of EPMs from the bulge area (g, arrows). Dotted line shows the basement membrane. Scale bars represent 25 μm in (g) and 5 μm in the inset of (g).

Figure S5. Kit^{+} pigmented cells in the hair follicle bulge are negative for CD11b (MAC1)

Immunohistochemical staining of anagen hair follicles for CD11b (MAC1) (a marker of monocytes, macrophages and cutaneous mast cells) (green) and for KIT (red). Bulge areas at

anagen IV of control follicles (a-f) and of irradiated hair follicles (g-l) are shown in bright field views (a, c, e, g, i and k) and immunostaining (b, d, f, h, j and l). Insets show magnified images of KIT^+ melanoblasts/melanocytes (b, h arrowheads) and KIT^+ $CD11b^+$cells (b, h, arrows). **a-f**, KIT^+ melanoblasts in the bulge areas of control follicles (a, b, arrowheads) did not contain any melanin pigment in the bright field view (a, c, arrowheads)**.** KIT^+ $CD11b^+$cells (a, b, and f, arrows) are located outside of the hair follicles. **g-l,** KIT^+ EPMs in the bulge areas of irradiated follicles (g, h, arrowheads). EPMs contain abundant pigment in the cytoplasm (g, i, arrowheads). KIT^+ $CD11b^+$cells (g, h, and l arrows) are located outside of the hair follicles and did not contain any pigment (k arrow). Dotted line shows the basement membrane. Scale bars represents 25 μm in (h) and 5 μm in the inset of (k and l).

Figure S6. Apoptosis is not the major fate of MSCs after IR at the dose sufficient for induction of hair graying.

Immunohistochemical staining of hair follicles for cleaved caspase3 (a-k, upper panel) (red) and for TUNEL activity (l-v, lower panel) (green) was not significantly increased in the bulge area including KIT^+ MSCs at any stages after IR (g-k, r-v), while cells in regressing hair bulbs of catagen II showed both cleaved caspase3 and TUNEL activity (f, q, white arrows). In irradiated follicles, KIT^+ cells are maintained in the bulge areas by anagen V and disappeared at anagen VI. Brackets indicate the bulge areas of hair follicles. Abbreviation: bb, hair bulb. Scale bars represents 100 μm in (f, q) and 200 μm in (k, v).

Figure S7. $p16^{INK4A}$ and p53 expression is undetectable in EPMs.

Immunohistochemical staining of $p16^{INK4A}$ and p53 (brown) in $lacZ^+$ EPMs (blue) in the bulge area of hair follicles. **a-g**, $p16^{INK4A}$ expression in bulge areas of hair follicles 5 days after 5 Gy IR

(b, d) or without (a, c) IR. Immunoreactivity with anti- $p16^{INK4A}$ antibody was undetectable in EPMs (b, arrowhead), while significant reactivity was found in the nuclei of keratinocytes in the transient portion of follicles and in lower bulge areas similarly with or without IR. No detectable difference in the immunoreactivity of p16 was found with or without IR. Significant expression of p16 was specifically found in human nevus nest (e, f) (positive control)

h-o, p53 expression in the hair follicle bulge at 3 days (k) and 5 days (m, o) after IR and in non-irradiated controls (j, l, n). Transient induction of p53 was observed in bulge areas at 3 days after IR (k), but became undetectable at 5 days after IR when EPMs were induced (m, o). p53 was induced in epidermal skin cells at 1 day after IR (i, positive control). Abbreviation: bg, bulge; sg, sebaceous gland. Scale bars represents 50 μm in (d), 10 μm in the inset of (d), 100 μm in (f, g), 20 μm in (i), and 25 μm in (k, o).

Figure S8. IR induces pigmentation and dendritic morphology in unpigmented human melanocytes *in vitro*.

a-f, Cell morphology changes of NHEMs after IR (5 Gy, c,d; 10 Gy, e,f) and in unirradiated controls (a,b). Highly pigmented melanocytes with bipolar or tripolar dendrites, and moderately pigmented polydendritic melanocytes were observed after IR. **g**, The frequency of melanin-containing NHEMs with or without IR. The white bar shows the non-irradiated control. The black bars show pigmented cells after IR. **h-k**, SA-β-Gal staining of irradiated NHEMs. The SA-β-Gal signal was observed in polydendritic melanocytes after IR (j and k), but not in a highly pigmented bipolar melanocyte, which resembles mouse EPMs (k arrowhead). **l-o**, γH2AX foci formation in NHEM after IR. Control NHEMs show bipolar cell bodies (l) and γH2AX foci formation was not found in these cells (m). Irradiated NHEMs shows dendritic cell bodies (n)

with γH2AX foci (o). Error bars represent SEM. *p < 0.001 as calculated by Student's t test. Scale bars represent 20 μm in (f) and 30 μm in (k, o).

Figure S9. Maturation of EPMs, but not MSC depletion nor hair graying, depends on Mc1r

a, b, Changes in coat color of control (a) or irradiated (b) *Mc1r*$^{e/e}$ mice 8 months after IR. **c-l,** KIT^{+} cells (green) in the bulge areas of wild type (*Mc1r*$^{E/E}$) (d-g) or *Mc1r*$^{e/e}$ mice (i-l) after various does of IR are shown in bright view images. KIT^{+} cells in the bulge area contain abundant black pigment (white arrowhead) in *Mc1r*$^{E/E}$ (f, g) but not in *Mc1R*$^{e/e}$ mice (k, l) after more than 5 Gy IR. Insets show magnified views of EPMs marked with white arrowheads (f, g). **m,** The frequency of hair follicle bulges containing Fontana-Masson (F-M) stained eu- or pheo-melanin producing cells in the bulge area per total hair follicles. **n-q**, Visualization of melanin deposits by F-M staining of the bulge (n, o) and control bulb areas (p, q). Small numbers of melanocytes with significantly low level of F-M^{+} melanin deposits are found in the bulge areas in *Mc1r*$^{e/e}$ (o), while mature melanocytes with abundant F-M^{+} deposits were frequently found in *Mc1r*$^{E/E}$ (n). Insets show magnified views of F-M^{+} EPMs indicated by arrowheads (n, o). **r-u,** Disappearance of lacZ^{+} cells in the hair follicle bulge of *Mc1r*$^{e/e}$ mice in the second hair cycle after IR. Whole mount (r, s) and sections of lacZ-stained control (t, u) and irradiated skin (r, t). Brackets indicate the bulge (bg) areas. LacZ^{+} cells were absent in the bulge areas of irradiated follicles (s, u). **v,** The frequency of hair follicles containing lacZ^{+} cells in the bulge area per total hair follicles in the 3rd hair cycles after IR. Scale bars represent 25 μm in (l, q)**,** 10 μm in the inset of (g, o), and 100 μm in (u). Error bars represent SEM.

Inomata_Figure S1

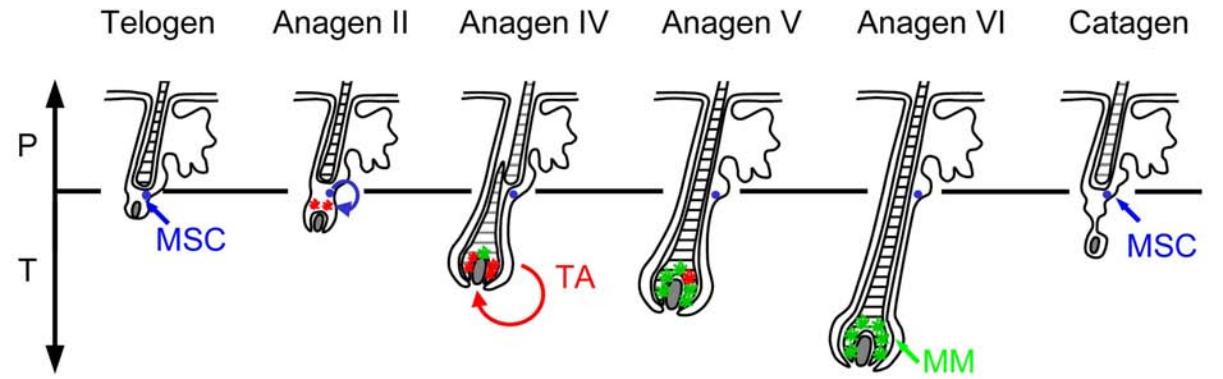

Inomata_Figure S2

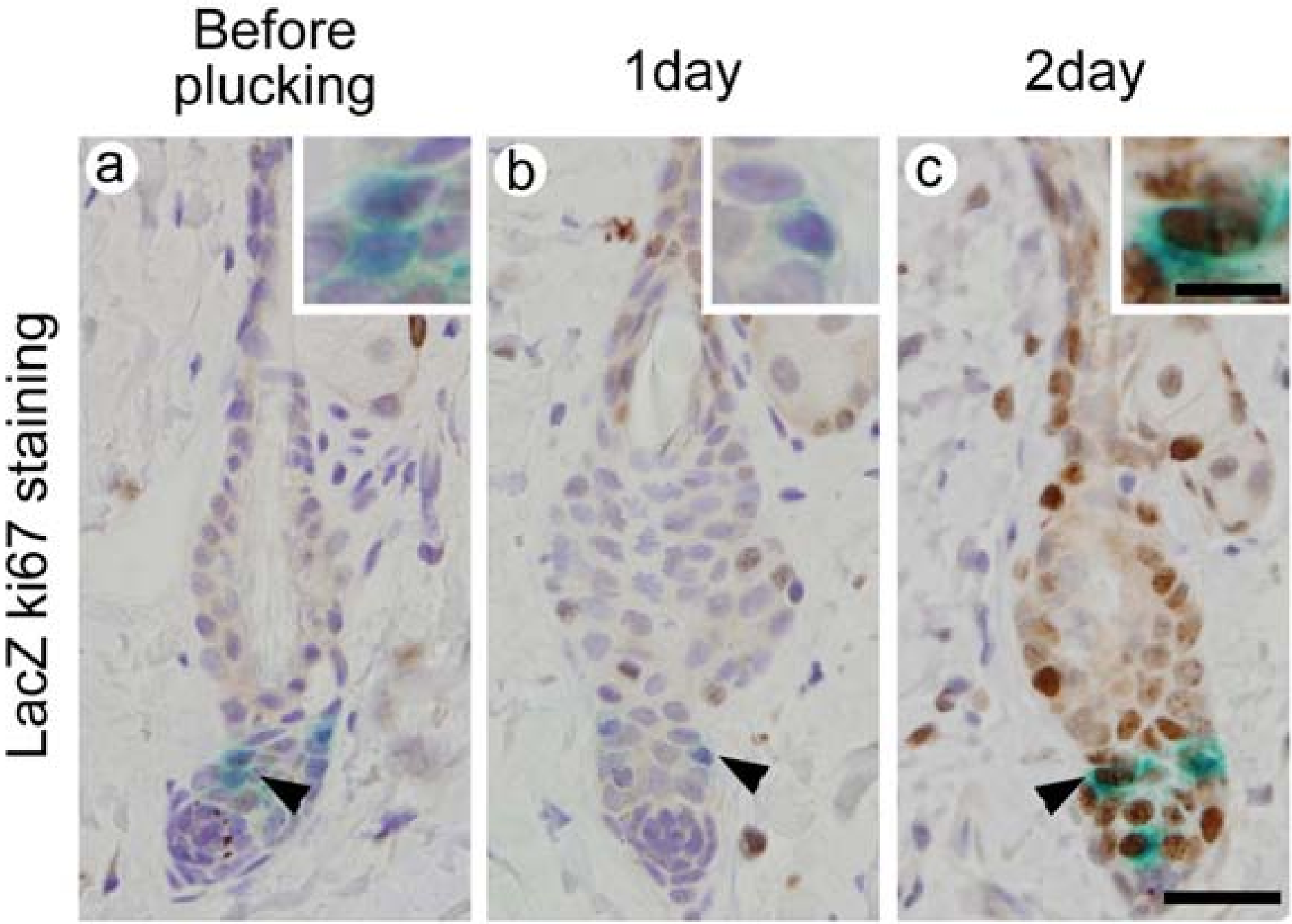

Inomata_Figure S3

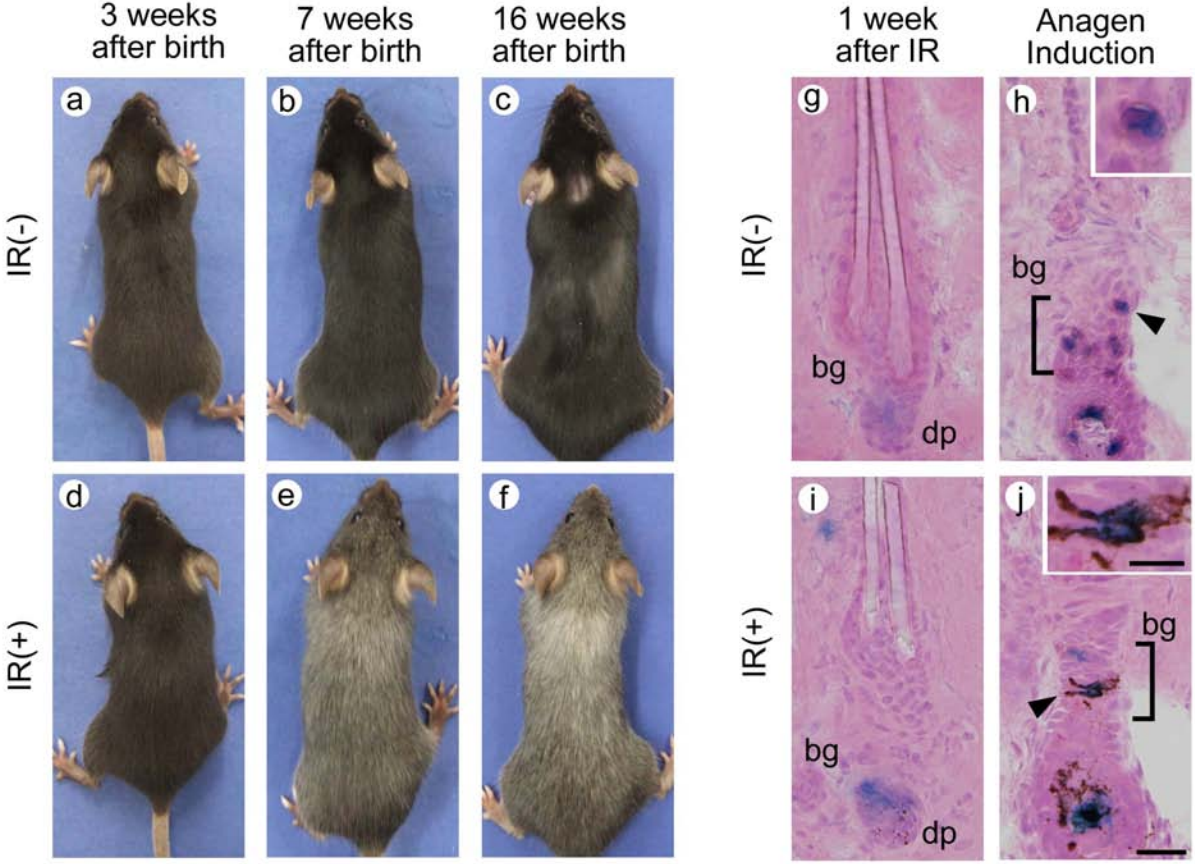

Inomata_Figure S4

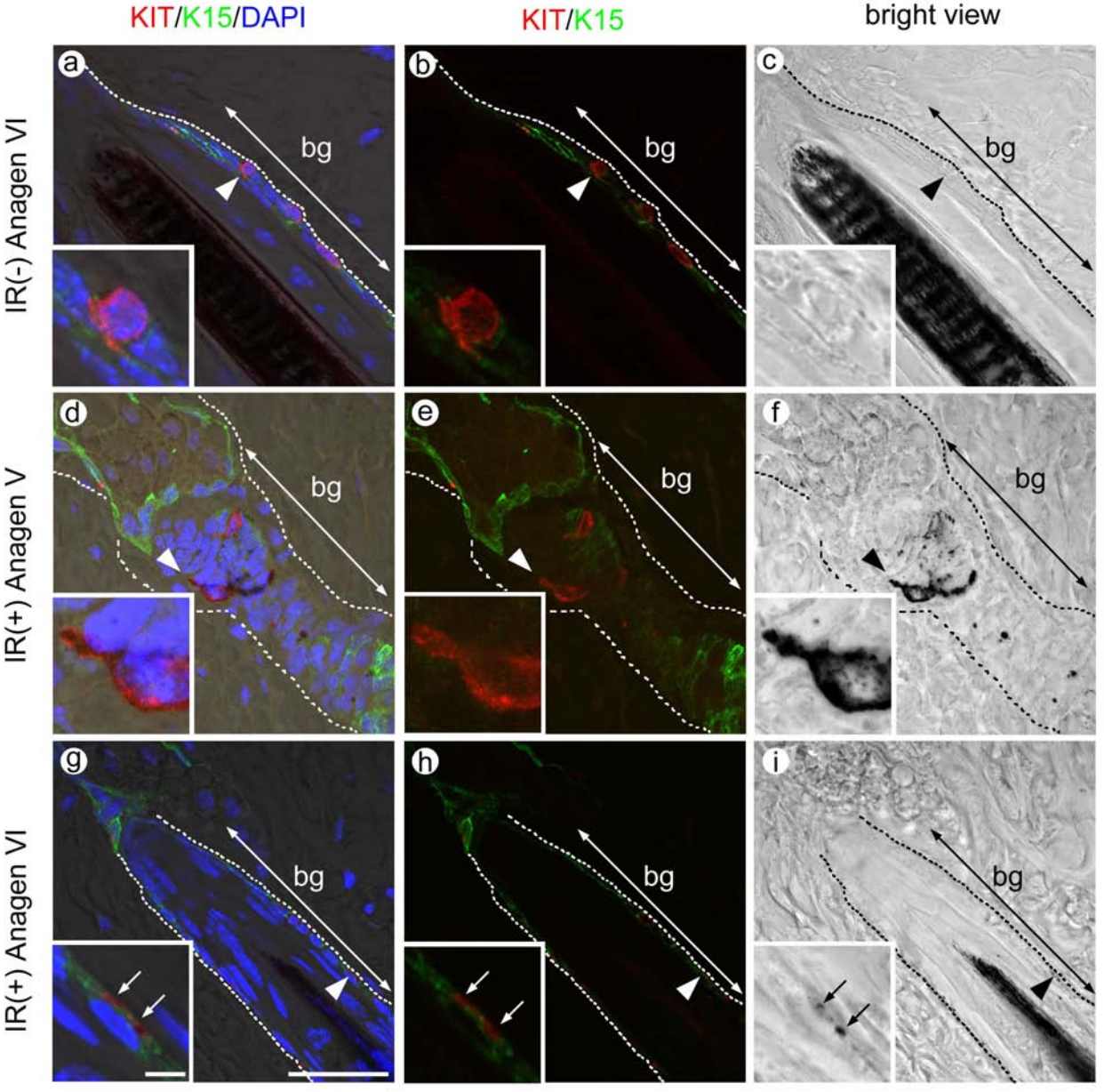

Inomata_Figure S5

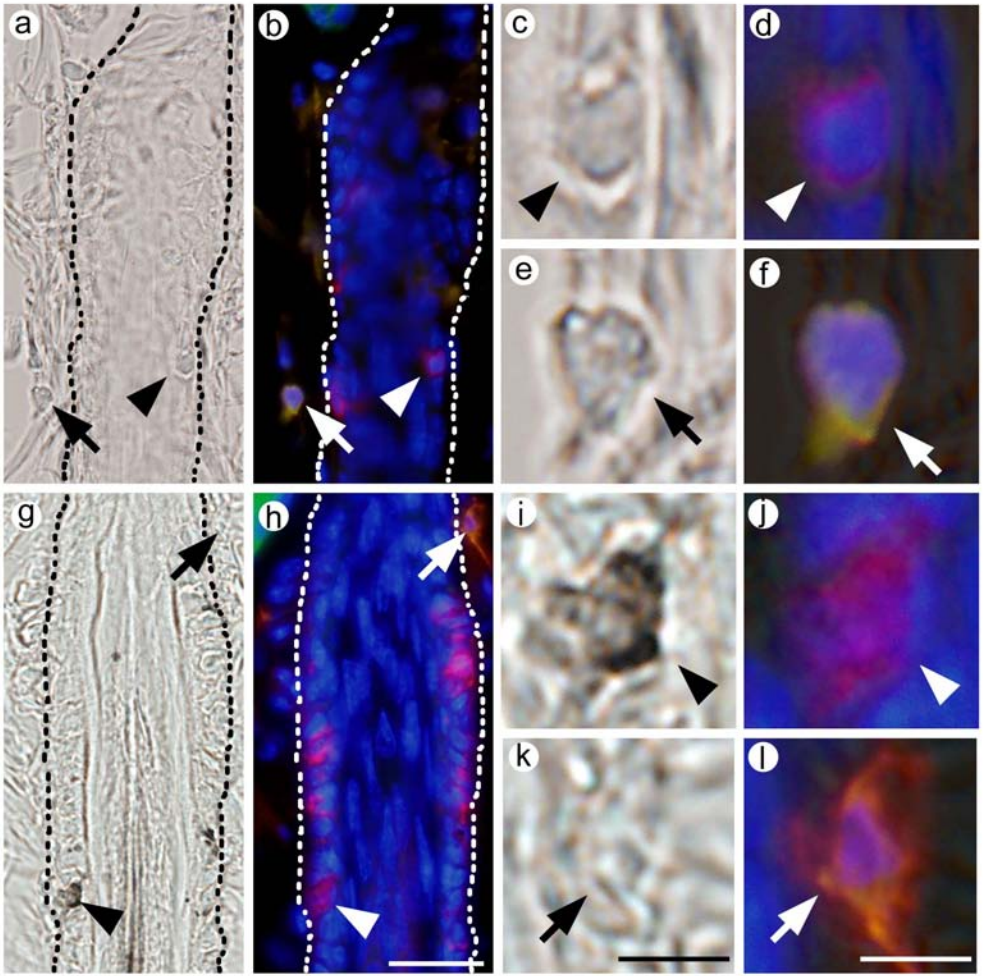

Inomata_Figure S6

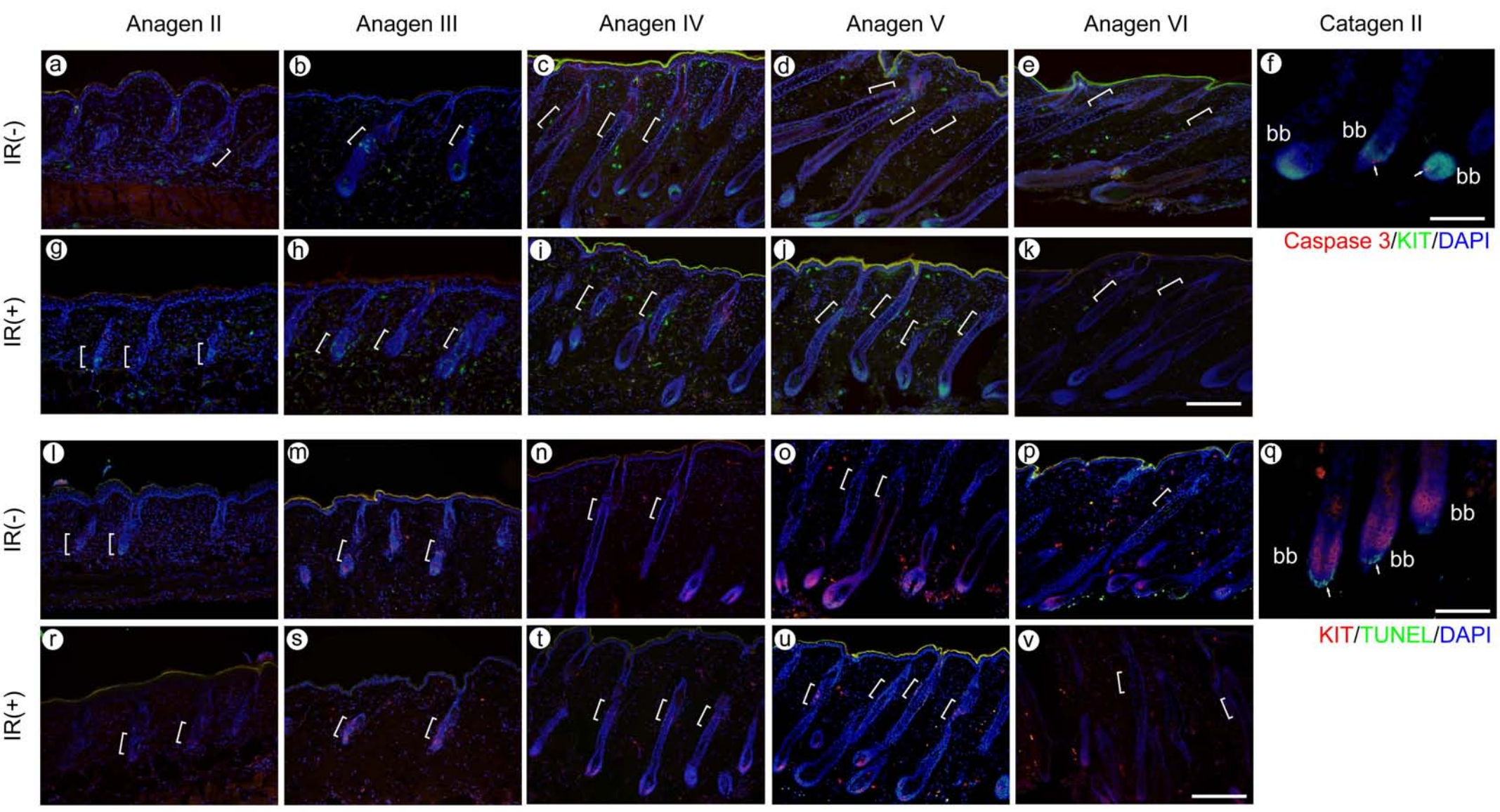

Inomata_Figure S7

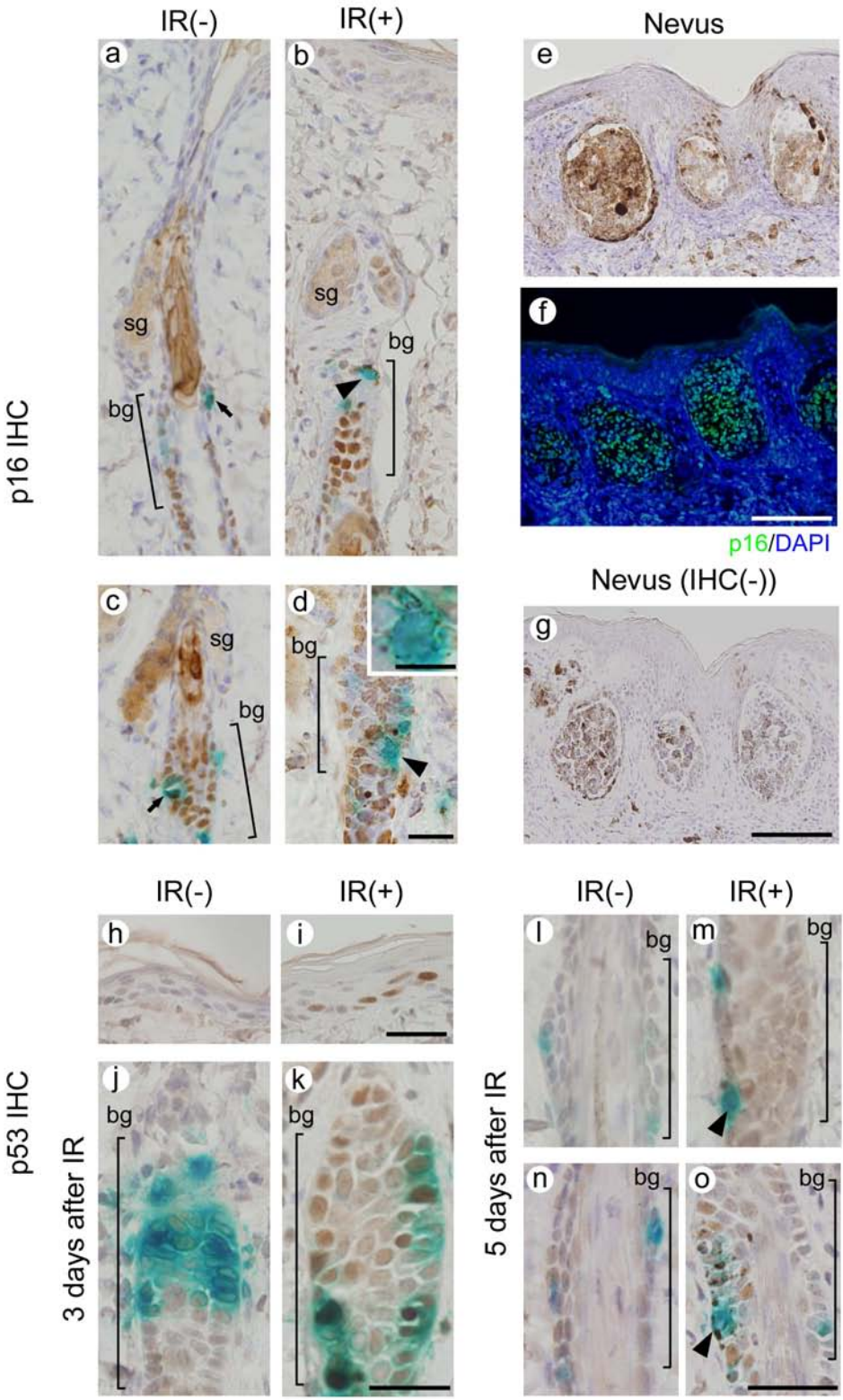

Inomata_Figure S8

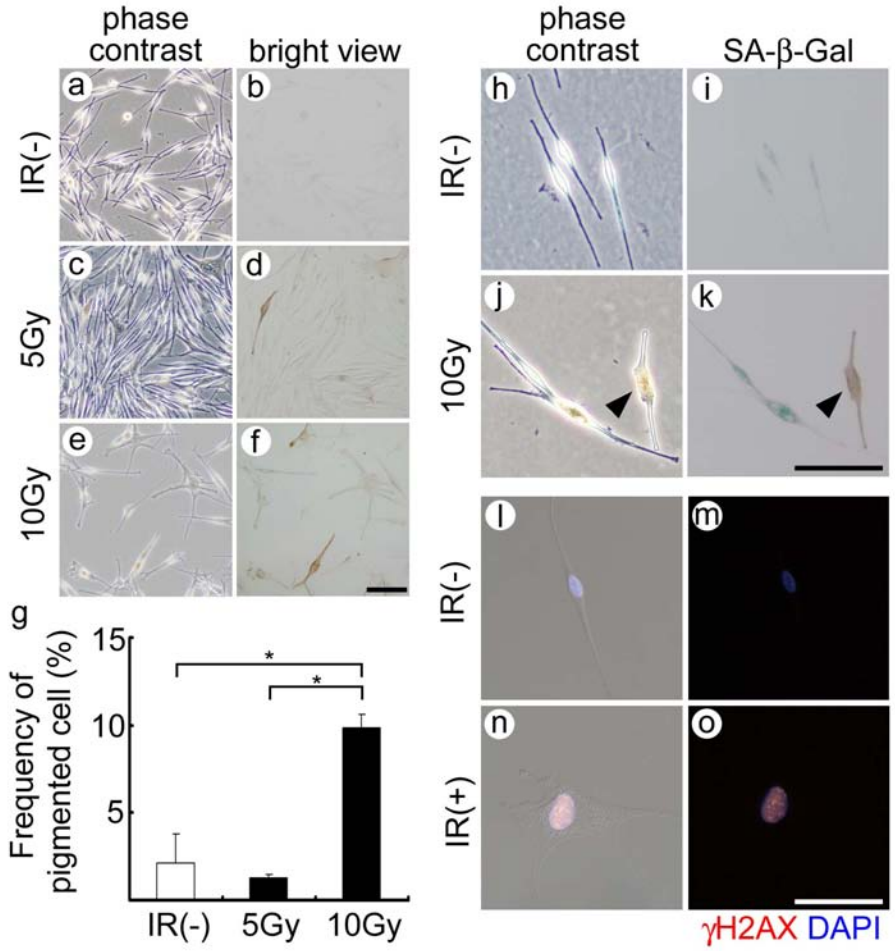

Inomata_Figure S9